JOURNAL OF DIFFERENTIAL EQUATIONS 135, 238–268 (1997)
ARTICLE NO. DE963237

Histogram Modification via Differential Equations

Guillermo Sapiro*

Hewlett-Packard Labs, 1501 Page Mill Road, Palo Alto, California 94304

and

Vicent Caselles†

Department of Mathematics and Informatics, University of Illes Balears, 07071 Palma de Mallorca, Spain

The explicit use of partial differential equations (PDEs) in image processing became a major research topic in the past years. In this work we present a framework for histogram (pixel-value distribution) modification via ordinary and partial differential equations. In this way, the image contrast is improved. We show that the histogram can be modified to achieve any given distribution as the steady state solution of an image flow. The contrast modification can be performed while simultaneously reducing noise in a unique PDE, avoiding noise sharpening effects of classical algorithms. The approach is extended to local contrast enhancement as well. A variational interpretation of the flow is presented and theoretical results on the existence of solutions are given. © 1997 Academic Press

1. INTRODUCTION

The use of ordinary and partial differential equations (ODEs and PDEs) for image processing became a major research topic in the past years. The first basic idea is not to think of image processing in the discrete domain but in the continuous one, and combine this with efficient numerical implementations. In general, let $\Phi_0: \mathbf{R} \times \mathbf{R} \to [0, M]$ represent a gray-level image, where $\Phi_0(x, y)$ is the gray-level value. That is, for each point (x, y) on the image (*pixel*), the value $\Phi_0(x, y)$ indicates its brightness, zero representing a black point and M, the maximal value, a white one. Color images are given in general by maps $\Phi_0: \mathbf{R} \times \mathbf{R} \to [0, M]^3$, where each scalar map represents one of the three colors red, green, and blue. In this

* E-mail: guille@hpl.hp.com.
† E-mail: dmivca0@ps.uib.es.

0022-0396/97 $25.00

paper, we deal mainly with gray-level images, maps from $\mathbf{R}^2$ to $\mathbf{R}$. The algorithms that we describe are based on the formulation of evolution type differential equations of the form

$$\frac{\partial \Phi}{\partial t} = \mathscr{F}[\Phi(x, y, t)],$$

where $\Phi(x, y, t): \mathbf{R}^2 \times [0, T) \to \mathbf{R}$ is the evolving image, $\mathscr{F}: \mathbf{R} \to \mathbf{R}$ is a given function which depends on the algorithm, and the image Φ_0 is the initial condition. The solution $\Phi(x, y, t)$ of the differential equation gives the processed image.

Most of the use of PDEs for image processing was done for image debluring or denoising, see for example [1, 2, 7, 14, 20, 24, 26, 30, 35, 36]. In this case, the basic idea is to perform anisotropic diffusion. That is, instead of applying to the image the flow

$$\frac{\partial \Phi}{\partial t} = \operatorname{div}(\nabla \Phi),$$

which is the classical heat equation, and will smooth the image in all directions (isotropic diffusion), destroying edges (points with high gradient $\|\nabla \Phi\|$), the common proposal is to use flows generated by a parabolic partial differential equation which penalizes the diffusion across the edges. (The original image Φ_0 is always taken as the initial condition of the corresponding PDEs.) The basic model is the so-called mean curvature motion equation

$$\frac{\partial \Phi}{\partial t} = \|\nabla \Phi\| \operatorname{div}\left(\frac{\nabla \Phi}{\|\nabla \Phi\|}\right), \tag{1}$$

which can be written in the form

$$\frac{\partial \Phi}{\partial t} = \Phi_{\xi\xi}, \tag{2}$$

where ξ is the direction perpendicular to the gradient $\nabla \Phi$, that is, parallel to the image edges. Thus, eliminating the diffusion across the edges in the heat equation model we formally arrive at the mean curvature model (1, 2). Related variational formulations lead to partial differential equations of the form

$$\frac{\partial \Phi}{\partial t} = \operatorname{div}(g(\|\nabla \Phi\|)\, \nabla \Phi) \tag{3}$$

where, again, smoothing across the edges can be avoided if g is a decreasing function. An important example is

$$\frac{\partial \Phi}{\partial t} = \operatorname{div}\left(\frac{\nabla \Phi}{\|\nabla \Phi\|}\right), \tag{4}$$

which is associated to the minimization of the Total Variation energy functional proposed in [30] and corresponds to $g(r) = 1/r$ in (3) (see also [7, 9, 13]). State of the art results have been obtained with these approaches. Let us mention that, for the general model (3), well-posedness is not guaranteed unless $G(r) = rg(r)$, $r \geqslant 0$, is a non decreasing function of r. This is one of the drawbacks of the Perona–Malik model [26] which motivated later research on anisotropic diffusion models, e.g., [2]. A systematic discussion of these fundamental smoothing processes can be found in [1].

An example of image denoising via PDEs is given in Fig. 1, taken from [23] (see also [1, 33, 34] and Section 3). In this example, an affine invariant version of the mean curvature equation (2), namely

$$\frac{\partial \Phi}{\partial t} = \|\nabla \Phi\| \operatorname{div}\left(\frac{\nabla \Phi}{\|\nabla \Phi\|}\right)^{1/3}, \tag{5}$$

is applied to a noisy image. Note how edges are preserved while the noise is removed.

This PDEs technique, mainly following the theory of curve evolution [12, 15, 22], was recently also used for a number of problems in computer vision as shape analysis [17, 25], recovery of shape from shading [18, 29], image segmentation [5, 6, 16, 21], invariant shape smoothing [1, 34], and mathematical morphology [1, 32]. In these flows, curves and images deform according to geometric measurements as curvature, while the deformation is also controlled by image-dependent external forces. Figure 2

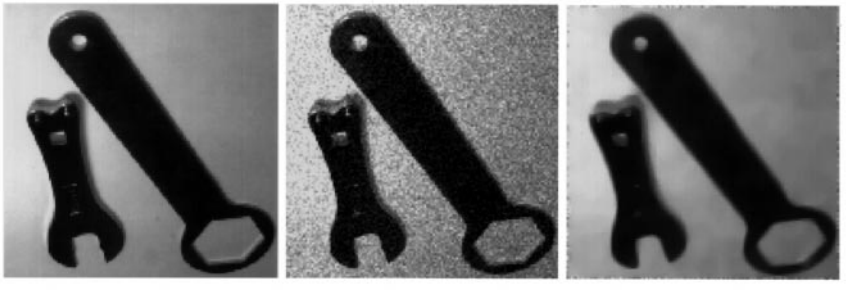

FIG. 1. Example of the (anisotropic) affine invariant image flow for image denoising and simplification. The original image is presented on the left, noisy on the middle, and reconstructed on the right.

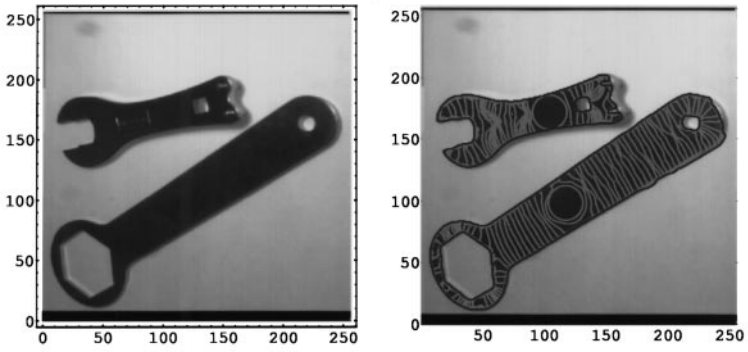

FIG. 2. Object detection via curvature based curve flows. The original curves are the two small circles inside the shapes, and they deform outward. The segmented objects are given by the final, steady state, dark curves.

shows an example of the curve evolution segmentation flow proposed in [6]. In this case, the curve deforms according to a function of its curvature and the gradient of the image, moving towards the objects to be detected in the gray-level image.

Advantages of this PDE technique have been already reported in [1, 31] and are supported by the previously mentioned papers. As we will see later in this paper and can be also appreciated for instance in [1, 2, 6, 16, 19, 24], the PDE approach provides a formal framework for image processing, allowing to prove important results as existence, uniqueness, and stability of solutions of the corresponding mathematical models. This kind of formal approach to image processing is quite unique.

An important characteristic of this technique is the natural way to combine algorithms. If two different procedures are given by

$$\frac{\partial \Phi}{\partial t} = \mathscr{F}_1[\Phi(x, y, t)], \qquad \frac{\partial \Phi}{\partial t} = \mathscr{F}_2[\Phi(x, y, t)],$$

then they can be combined as

$$\frac{\partial \Phi}{\partial t} = \alpha \mathscr{F}_1[\Phi(x, y, t)] + \mathscr{F}_2[\Phi(x, y, t)],$$

where $\alpha \in \mathbf{R}^+$. This was successfully used for example in [3], where $\mathscr{F}_1$ was the smoothing operator in [2] and $\mathscr{F}_2$ the debluring one in [24]. Note that variational approaches are also natural for this type of algorithms combination, where in this case the combined scheme is obtained by adding the different energies. This will be exploited later in this paper.

The theories developed in the above mentioned papers, as well as in this one, are initially formulated in the continuous domain. In practice, images are digitized, which means that their values are given only on a discrete grid of a rectangle. However, it is very convenient to discuss the geometry of images in the continuous framework of functional analysis. This passage is justified provided it is shown that the algorithms defined in the continuous model can be made effective in their digitized trace. Indeed one of the advantages of this methodology is the accuracy achieved when efficient numerical implementations are used. This makes the algorithms very appropriate for example for medical applications.

To deal with the natural discontinuities of images, in [1, 2], the authors introduced the framework of viscosity solutions [9] into the area of PDEs in image processing. This framework was developed for related surface evolution equations for example in [8, 10], as well as for image processing flows in [1, 5, 6, 16]. In the PDE formulation, to give a classical mathematical sense to models like (1, 5), the initial image needs to be a continuous function. One can object that this is not a realistic requirement for images. Images have, of course, discontinuities. As was done in [1, 2], we may assume that these discontinuities are steep edges which may be justified by saying that both things are equivalent at the discrete level. In addition, variational models like those based on Total Variation permit to work with discontinuous data (functions of bounded variation), as for example natural images ([7, 19]).

Let us now present the purpose of this paper. Images are captured at low contrast in a number of different scenarios. The main reason for this is wrong lighting conditions. As a result, the image looks too dark, or too bright, and is inappropriate for visual inspection or observation. The most common way to improve the contrast of an image is to modify its pixel value distribution, or *histogram*. In this work we present a novel image flow for gray-level histogram modification. In Fig. 3 we show an example of this. The image on the left is the original, low contrast one, while the one on the right is obtained with one of the options for contrast enhancement presented in this paper. Note how many objects that are not seen on the original image are easily detected in the processed one. More examples will be given later in this paper.

We initially show how to obtain any gray-level distribution as the steady state of an ODE, and present examples for different pixel value distributions. Uniform distributions are usually used in most contrast enhancement applications. On the other hand, for specific tasks, the exact desirable distribution can be dictated by the application, and the technique here presented applies as well. After this basic equation is presented and analized, we combine it with the smoothing operators proposed in [35] and in [30], obtaining contrast normalization and denoising at the same

FIG. 3. Example of contrast enhancement. Note how objects that are not visible on the original image on the left (e.g., the 2nd chair and the objects trough the window), are now detectable in the processed one (right).

time. We also extend the flow to local contrast enhancement both in the image plane and in the gray-value space. Local contrast enhancement in the gray-value space is performed for example to improve the visual appearance of the image (the reason for this will be explained latter in the paper). We should mention that the straightforward extension of our formulation to local contrast enhancement in the image domain, that is, in the neighborhood of each pixel, does not achieves good results. Indeed, in this case, fronts parallel to the edges are created (this is common to most contrast enhancement techniques). At the experimental level, one can avoid this by combining local and global techniques in the framework here presented.

After giving the basic image flows for histogram modification, a variational interpretation of the histogram modification flow and theoretical results regarding existence of solutions to the proposed equations are presented.

We should point out that in [27] the authors recently presented a diffusion network for image normalization. In their work, the image $\Phi(x, y)$ is normalized via

$$\frac{\Phi - \Phi_a}{\Phi_M - \Phi_m},$$

where Φ_a, Φ_M, and Φ_m are the average, maximum, and minimum of Φ over local areas. These values are computed using a diffusion flow, which minimizes a cost functional. The method was generalized computing a full local frame of reference for the gray level values of the image. This is achieved changing the variables in the flow. A number of properties, including existence of the solution of the diffusion flow, were presented

as well. In contrast with their work, in our case we have full control of the final distribution of the gray-levels, that means while their work is on contrast normalization, our is on histogram modification. Also, the modified image is obtained in this work as the steady state solution of the flow, without any extra operations as required in [27]. This allows straightforward combination with other PDEs based algorithms as explained above. No energy-type interpretation is given in [27].

Before proceeding with the technical details, let us remark the main advantages of the contrast enhancement framework described in this paper. All the points will be further explained later in the paper. Basically, the approach here described has the following characteristics:

1. Presents contrast enhancement as an image deformation algorithm and not just as a distribution modification one. This progressively improves the contrast, allowing as well to choose intermediate steps.

2. Enriches the area of PDEs in image processing, showing how to solve one of the most important problems in image processing via image flows.

3. Makes it possible to perform contrast enhancement and denoising simultaneously.

4. Presents a variational framework for contrast enhancement, formulated in the image domain. This permits to improve classical techniques, including for example image and perceptual models, as well as to better understand current approaches.

5. Holds formal existence (and uniqueness) results.

2. HISTOGRAM MODIFICATION

As explained in the Introduction, the most common way to improve the contrast of an image is to modify its pixel value distribution, i.e., the histogram. We shall do this by means of an evolution equation. We start with the equation for histogram equalization, and then we extend it for any given distribution. In histogram equalization, the goal is to achieve an uniform distribution of the image values [28]. That means, given the gray-level distribution p of the original image, the image values are mapped into new ones such that the new distribution $\hat{p}$ is uniform. In the case of digital images, $p(i)$, $0 \leqslant i \leqslant M$, is computed as

$$p(i) = \frac{\text{Number of pixels with value } i}{\text{Total number of pixels in the image}},$$

and uniformity can be obtained only approximately.

We proceed to show an image evolution equation that achieves this uniform distribution when it arrives to steady state. Assume that the continuous image $\Phi(x, y, t)$: $[0, N]^2 \times [0, T) \to [0, M]$ evolves according to

$$\frac{\partial \Phi(x, y, t)}{\partial t} = (N^2 - N^2/M\, \Phi(x, y, t)) - \mathscr{A}[(v, w): \Phi(v, w, t) \geqslant \Phi(x, y, t)], \tag{6}$$

where $\mathscr{A}[\cdot]$ represents area (or number of pixels in the discrete case). For the steady state solution ($\Phi_t = 0$) we have

$$\mathscr{A}[(v, w): \Phi(v, w) \geqslant \Phi(x, y)] = (N^2 - N^2/M\, \Phi(x, y)).$$

Then, for $a, b \in [0, M]$, $b > a$, we have

$$\mathscr{A}[(v, w): b \geqslant \Phi(v, w) \geqslant a] = (N^2/M) * (b - a),$$

which means that the histogram is constant. Therefore, the steady state solution of (6), if it exists (see below), gives the image after normalization via histogram equalization.

From (6) we can extend the algorithm to obtain any given gray-value distribution h: $[0, M] \to \mathbf{R}^+$. Let $H(s) := \int_0^s h(\xi)\, d\xi$. That is, $H(s)$ gives the density of points between 0 and s. Then, if the image evolves according to

$$\frac{\partial \Phi(x, y, t)}{\partial t} = (N^2 - H[\Phi(x, y, t)]) - \mathscr{A}[(v, w): \Phi(v, w, t) \geqslant \Phi(x, y, t)], \tag{7}$$

the steady state solution is given by

$$\mathscr{A}[(v, w): \Phi(v, w) \geqslant \Phi(x, y)] = (N^2 - H[\Phi(x, y)]).$$

Therefore,

$$\mathscr{A}[(v, w): \Phi(x, y) \leqslant \Phi(v, w) \leqslant \Phi(x, y) + \delta] = H[\Phi(x, y) + \delta] - H[\Phi(x, y)]),$$

and taking Taylor expansion when $\delta \to 0$ we obtain the desired result. Note that of course (6) is a particular case of (7), with $h = \text{constant}$.

2.1. *Existence and Uniqueness of the Flow*

We present now results related to the existence and uniqueness of the proposed flow for histogram equalization. We will see that the flow for

histogram modification has an explicit solution, and its steady state is straightforward to compute. This is due to the fact, as we will prove below, that the value of $\mathscr{A}$ is constant in the evolution. This is not unexpected, since it is well known that histogram modification can be performed with look-up tables. In spite of this, it is important, and not only from the theoretical point of view, to first present the basic flow for histogram modification, in order to arrive to the energy based interpretation and to derive the extensions presented later in this paper. These extensions do not have explicit solutions.

Let Φ_0 be an image, i.e., a bounded measurable function, defined in $[0, N]^2$ with values in the range $[a, b]$, $0 \leqslant a < b \leqslant M$. We assume that the distribution function of Φ_0 is continuous, that is

$$\mathscr{A}[X: \Phi_0(X) = \lambda] = 0 \tag{8}$$

for all $X \in [0, N]^2$ and all $\lambda \in [a, b]$. To equalize the histogram of Φ_0 we look for solutions of

$$\Phi_t(t, X) = \mathscr{A}[Z: \Phi(t, Z) < \Phi(t, X)] - \frac{N^2}{b-a}(\Phi(t, X) - a) \tag{9}$$

which also satisfy

$$\mathscr{A}[X: \Phi(t, X) = \lambda] = 0. \tag{10}$$

Hence the distribution function of $\Phi(t, X)$ is also continuous. This requirement, mainly technical, avoids the possible ambiguity of changing the sign "$<$" by "$\leqslant$" in the computation of $\mathscr{A}$ (see also the remarks at the end of this section).

Let us recall the definition of $\operatorname{sign}^-(\cdot)$:

$$\operatorname{sign}^-(r) = \begin{cases} 1 & \text{if} \quad r < 0 \\ [0, 1] & \text{if} \quad r = 0 \\ 0 & \text{if} \quad r > 0. \end{cases}$$

With this notation, Φ satisfying (9) and (10) may be written as

$$\Phi_t(t, X) = \int_{[0, N]^2} \operatorname{sign}^-(\Phi(t, Z) - \Phi(t, X))\, dZ - \frac{N^2}{b-a}(\Phi(t, X) - a). \tag{11}$$

Observe that as a consequence of (10), the real value of sign^- at zero is unimportant, avoiding possible ambiguities. In order to simplify the

notation, let us normalize Φ such that it is defined on $[0, 1]^2$ and takes values in the range $[0, 1]$. This is done just by the change of variables given by

$$\Phi(t, X) \leftarrow \frac{\Phi(\mu t, NX) - a}{b - a},$$

where $\mu = (b - a)/N^2$. Then, Φ satisfies the equation

$$\Phi_t(t, X) = \int_{[0, 1]^2} \text{sign}^-(\Phi(t, Z) - \Phi(t, X))\, dZ - \Phi(t, X). \tag{12}$$

Therefore, without loss of generality we can assume $N = 1$, $a = 0$, and $b = 1$, and analyze (12). Let us make precise our notion of solution for (12).

DEFINITION 1. A bounded measurable function $\Phi: [0, \infty) \times [0, 1]^2 \to [0, 1]$ will be called a solution of (12) if, for almost all $X \in [0, 1]^2$, $\Phi(\cdot, X)$ is continuous in $[0, \infty)$, $\Phi_t(\cdot, X)$ exists a.e. with respect to t and (12) holds a.e. in $[0, \infty) \times [0, 1]^2$.

Now we may state the following result:

THEOREM 1. *For any bounded measurable function $\Phi_0: [0, 1]^2 \to [0, 1]$ such that $\mathscr{A}[Z: \Phi_0(Z) = \lambda] = 0$ for all $\lambda \in [0, 1]$, there exists a unique solution $\Phi(t, X)$ in $[0, \infty) \times [0, 1]^2$ with range in $[0, 1]$ satisfying the flow (12) with initial condition given by Φ_0, and such that $\mathscr{A}[Z: \Phi(t, Z) = \lambda] = 0$ for all $\lambda \in [0, 1]$. Moreover, as $t \to \infty$, $\Phi(t, X)$ converges to the histogram equalization of $\Phi_0(X)$.*

Proof. We start with the existence. We look for a solution $\Phi(t, X)$ such that

$$\mathscr{A}[Z: \Phi(t, Z) < \Phi(t, X)] = \mathscr{A}[Z: \Phi(0, Z) < \Phi(0, X)]. \tag{13}$$

This assumption is enough to prove existence. This will also mean that a closed solution exists for (12), further supporting the validity of the proposed image flow. Note that having $\mathscr{A}$ constant in time transforms the equation into a family of ODEs, one for each space coordinate (x, y) (this is generally true for histogram modification techniques, since they are based on pixel value distributions). In spite of this, which makes the original equation as trivial as classical histogram equalization techniques, the formulation is crucial for later sections, where local and simultaneous contrast enhancement and denoising models are presented. For those models, which do not have a closed solution, it is important to identify the

basic histogram modification algorithm. Moreover, we will later prove that condition (13) actually holds for any solution of (12).

Thus, let $\mathscr{F}_0(X) := \mathscr{A}[Z: \Phi(t, Z) < \Phi(t, X)]$, which is independent of t. Then, (12) can be re-written as

$$\Phi_t = \mathscr{F}_0(X) - \Phi(t, X), \tag{14}$$

whose explicit solution is

$$\Phi(t, X) = \exp\{-t\}\ \Phi_0 + (1 - \exp\{-t\})\ \mathscr{F}_0(X), \tag{15}$$

which satisfies

$$\mathscr{A}[Z: \Phi(t, Z) = \lambda] = 0, \qquad t \geqslant 0, \quad \lambda \in [0, 1]. \tag{16}$$

Observe that our solution is a continuous function of t for all X and satisfies

$$\Phi(t, X) < \Phi(t, X') \qquad \text{if and only if} \quad \Phi_0(X) < \Phi_0(X') \tag{17}$$

for all $t > 0$ and all $X, X' \in [0, 1]^2$. That is, the grey-value order is preserved. Observe also that $[0, 1]$ is the smallest interval which contains the range of the solution. As $t \to +\infty$, $\Phi(t, X) \to \mathscr{F}_0(X)$. It is easy to see that the distribution function of $\mathscr{F}_0(X)$ is uniform.

Note that equation (15) progressively improves the image contrast, until steady state is achieved. This gives an advantage over classical histogram equalization, where intermediate "contrast states" are not available, and if the solution has excessive contrast, there is no possible compromise.

In order to prove uniqueness, we need to following lemma:

LEMMA 1. *Let $\Phi(t, X)$ be a solution of* (12). *Let $X, X' \in [0, 1]^2$ be such that $\Phi(\cdot, X)$, $\Phi(\cdot, X')$ are continuous in $[0, \infty)$, $\Phi_t(\cdot, X)$, $\Phi_t(\cdot, X')$ exist a.e. with respect to t and* (12) *holds a.e. in t. Suppose that $\Phi(0, X) < \Phi(0, X')$. Then*

$$\Phi(t, X') - \Phi(t, X) \geqslant \exp\{-t\}(\Phi(0, X') - \Phi(0, X)) \qquad \textit{for all} \quad t \geqslant 0. \tag{18}$$

Proof. Let $\delta > 0$. Then, using our assumptions,

$$\begin{aligned}
&\frac{d}{dt}\left(-\frac{1}{2}\ln(\delta^2 + (\Phi(t, X') - \Phi(t, X))^2\right) \\
&= \frac{\Phi(t, X) - \Phi(t, X')}{\delta^2 + (\Phi(t, X') - \Phi(t, X))^2}\left(\int \operatorname{sign}^-(\Phi(t, Z) - \Phi(t, X'))\, dZ\right. \\
&\quad \left. - \int \operatorname{sign}^-(\Phi(t, Z) - \Phi(t, X))\, dZ\right) + \frac{(\Phi(t, X') - \Phi(t, X))^2}{\delta^2 + (\Phi(t, X') - \Phi(t, X))^2}.
\end{aligned}$$

One easily verifies that the first term above is negative. Therefore

$$\frac{d}{dt}\left(-\frac{1}{2}\ln(\delta^2+(\Phi(t,X')-\Phi(t,X))^2\right)\leqslant\frac{(\Phi(t,X')-\Phi(t,X))^2}{\delta^2+(\Phi(t,X')-\Phi(t,X))^2}\leqslant 1.$$

After integration we observe

$$\sqrt{\delta^2+(\Phi(t,X')-\Phi(t,X))^2}\geqslant\exp\{-t\}\ \sqrt{\delta^2+(\Phi(0,X')-\Phi(0,X))^2}.$$

Letting $\delta\to 0$,

$$|\Phi(t,X')-\Phi(t,X)|\geqslant\exp\{-t\}\ |\Phi(0,X')-\Phi(0,X)|>0.$$

Since $\Phi(t,X)$, $\Phi(t,X)$ are continuous, this implies (18). ▮

Let $\Phi(t,X)$ be a solution of (12). As a consequence of the previous lemma we have

$$\begin{aligned}[Z\colon \Phi(0,Z)<\Phi(0,X)]&\subseteq[Z\colon \Phi(t,Z)<\Phi(t,X)]\\&\subseteq[Z\colon \Phi(0,Z)\leqslant\Phi(0,X)]\\[Z\colon \Phi(t,Z)=\Phi(t,X)]&\subseteq[Z\colon \Phi(0,Z)=\Phi(0,X)]\end{aligned}$$

for almost all $X\in[0,1]^2$. Since $\mathscr{A}[Z\colon \Phi(0,Z)=\lambda]=0$, we also have $\mathscr{A}[Z\colon \Phi(t,Z)=\lambda]=0$, for all $\lambda\in[0,1]$, and it follows that

$$\begin{aligned}&\int \operatorname{sign}^-(\Phi(t,Z)-\Phi(t,X))\,dZ\\&=\int \operatorname{sign}^-(\Phi(0,Z)-\Phi(0,X))\,dZ=\mathscr{T}_0(X).\end{aligned}$$

The flow can be re-written as (14), and (15) gives the solution. Uniqueness follows. Letting $t\to\infty$, $\Phi(t,X)$ tends to $\mathscr{T}_0(X)$, which corresponds to the equalized histogram for $\Phi_0(X)$. ▮

Remarks. 1. Even if the initial image Φ_0 is not continuous it may happen that $\mathscr{T}_0(X)$ is continuous. Hence an edge may disappear. This is a limitation of both this and the classical methods of histogram equalization. In spite of possible *ad hoc* solutions, the problem requires a sound formulation and solution. We are currently working on using the framework developed in this paper to investigate shape preserving contrast enhancement techniques.

2. According to our assumption (10), the initial image cannot take a constant value in a region of positive area. (Note that this assumption is only in order to present the theoretical results. The image flow and its basic

contrast modification characteristics remain valid also when (10) is violated.) If we expect as final result an image whose grey level distribution is perfectly uniform, we must assume (10) unless we admit that the same grey level can be mapped to different grey levels. In practice, perfect uniform is not necessary, and assumption (10) does not bring a mayor difficulty.

3. The above proof can be adapted to any required gray-value distribution h as the above result can be extended for the flow

$$\Phi_t(t, X) = \int \text{sign}^-(\Phi(t, Z) - \Phi(t, X))\, dZ - \Psi(\Phi(t, X)), \tag{19}$$

where Ψ is any strictly increasing Lipschitz continuous function. This allows to obtain any desired distribution. As pointed out before, the specific distribution depends on the application. Uniform distributions are the most common choice. If it is known in advance for example that the most important image information is between certain gray-value region, h can be such that it allows this region to expand further, increasing the detail there. Another possible way of finding h is to equalize between local minima of the original histogram, preserving certain type of structure in the image.

2.2. *Variational Interpretation of the Histogram Flow*

The formulation given by equations (11) and (12) not only helps to prove the theorem above, also gives a variational interpretation of the histogram modification flow. Variational approaches are frequently used in image processing. They give explicit solutions for a number of problems, and very often help to give an intuitive interpretation of this solution, interpretation which is many times not so easy to achieve from the corresponding Euler–Lagrange or PDE. Variational formulations help to derive new approaches to solve the problem as well.

Let us consider the following functional

$$\mathcal{U}(\Phi) = \tfrac{1}{2} \int (\Phi(X) - \tfrac{1}{2})^2\, dX - \tfrac{1}{4} \iint |\Phi(X) - \Phi(Z)|\, dX\, dZ, \tag{20}$$

where $\Phi \in L^2[0, 1]^2$, $0 \leqslant \Phi(X) \leqslant 1$. $\mathcal{U}$ is a Lyapounov functional for the equation (12):

LEMMA 2. *Let Φ be the solution of* (12) *with initial data Φ_0 as in Theorem* 1. *Then*

$$\frac{d\mathcal{U}(\Phi)}{dt} \leqslant 0.$$

Proof.

$$\frac{d\mathscr{U}(\Phi)}{dt} = \int (\Phi(X) - \tfrac{1}{2})\, \Phi_t(X)\, dX$$

$$-\tfrac{1}{4} \iint \operatorname{sign}(\Phi(Z) - \Phi(X))(\Phi_t(Z) - \Phi_t(X))\, dX\, dZ.$$

Let's denote the first integrand in the equation above by A and the second by B. Observe that due to (16), part B of the integral above is well defined. Let us re-write B as

$$B = \tfrac{1}{4} \iint \operatorname{sign}(\Phi(Z) - \Phi(X))\, \Phi_t(Z)\, dX\, dZ$$

$$-\tfrac{1}{4} \iint \operatorname{sign}(\Phi(Z) - \Phi(X))\, \Phi_t(X)\, dX\, dZ.$$

Interchanging the variables X and Z in the first part of the expression above we obtain

$$B = -\tfrac{1}{2} \iint \operatorname{sign}(\Phi(Z) - \Phi(X))\, \Phi_t(X)\, dX\, dZ.$$

Fixing X we have

$$\int \operatorname{sign}(\Phi(t, Z) - \Phi(t, X))\, dZ = 1 - 2 \int \operatorname{sign}^-(\Phi(t, Z) - \Phi(t, X))\, dZ,$$

and we may write

$$B = -\tfrac{1}{2} \int \Phi_t(X)\, dX + \iint \operatorname{sign}^-(\Phi(Z) - \Phi(X))\, \Phi_t(X)\, dZ\, dX.$$

Hence

$$\frac{d\mathscr{U}(\Phi)}{dt} = \int \Phi(t, X)\, \Phi_t(t, X)\, dX$$

$$-\iint \operatorname{sign}^-(\Phi(t, Z) - \Phi(t, X))\, \Phi_t(t, X)\, dX\, dZ$$

$$= \int \left\{ \Phi(t, X) - \int \operatorname{sign}^-(\Phi(t, Z) - \Phi(t, X))\, dZ \right\} \Phi_t(t, X)\, dX$$

$$= -\int \Phi_t(t, X)^2\, dX \leqslant 0.$$

This concludes the proof. ∎

Therefore, when solving (12) we are indeed minimizing the functional $\mathcal{U}$ given by (20) restricted to the condition that the minimizer satisfies (16).

This variational formulation gives a new interpretation to histogram modification and contrast enhancement in general. It is important to note that in contrast with classical techniques of histogram modification, it is completely formulated in the image domain and not in the probability one (although the spatial relation of the image values is still not important, until the formulations below). The first term in $\mathcal{U}$ stands for the "variance" of the signal, while the second one gives the contrast between values at different positions. To the best of our knowledge, this is the first time a formal image based interpretation to histogram equalization is given, showing the effect of the operation to the image contrast.

From this formulation, other functionals can be proposed to achieve contrast modification while including image and perception models. One possibility is to change the metric which measures contrast, second term in the equation above, by metrics which better model for example visual perception. It is well known that the total absolute difference is not a good perceptual measurement of contrast in natural images. At least, this absolute difference should be normalized by the local average. This also explains why ad-hoc techniques that segment the grey-value domain and perform (independent) local histogram modification in each one of the segments perform better than global modifications. This is due to the fact that the normalization term is less important when only pixels of the same range value are considered. Note that doing this is straightforward in our framework, $\mathcal{A}$ should only consider pixels in between certain range in relation with the value of the current pixel being updated.

From the variational formulation is also straightforward to extend the model to local (in image space) enhancement by changing the limits in the integral from global to local neighborhoods. In the differential form, the corresponding equations is

$$\frac{\partial \Phi}{\partial t} = (N^2 - H[\Phi(x, y, t)]) - \mathcal{A}[(v, w) \in \mathrm{B}(v, w, \delta) : \Phi(v, w, t) \geqslant \Phi(x, y, t)], \tag{21}$$

where $\mathrm{B}(v, w, \delta)$ is a ball of center (v, w) and radius δ ($\mathrm{B}(v, w)$ can also be any other surrounding neighborhood, obtained from example from previously performed segmentation). The main goal of this type of local contrast enhancement is to enhance the image for object detection. This formulation does not work perfectly in practice when the goal of the contrast enhancement algorithm is to obtain a visually pleascent image. Fronts parallel to the edges are created as we can see in Fig. 7. (Further

experiments with this model are presented in Section 4.) Effects of the local model can be moderated by combining it with the global model.

Based on the same approach, it is straightforward to derive models for contrast enhancement of movies, integrating over corresponding zones in different frames, when correspondence could be given, for example, by optical flow. Another advantage is the possibility to combine it with other operations. As an example, in the next section, an additional smoothing term will be added to the model (12).

3. SIMULTANEOUS ANISOTROPIC DIFFUSION AND HISTOGRAM MODIFICATION

We present now a flow for simultaneous de-noising and histogram modification. This is just an example of the possibility of combining different algorithms in the same PDE.

In [35], we presented a geometric flow for edge preserving anisotropic diffusion, based on the results in [1, 2] and [33, 34]. The basic idea, briefly describe in the Introduction, is to smooth the image only in the direction parallel to the edges, achieving this via curvature flows. The flow is given by

$$\frac{\partial \Phi}{\partial t} = \frac{1}{1 + \|\nabla(G * \Phi)\|} \kappa^{1/3} \|\nabla \Phi\|, \tag{22}$$

which is equivalent to

$$\frac{\partial \Phi}{\partial t} = \frac{1}{1 + \|\nabla(G * \Phi)\|} (\Phi_x^2 \Phi_{yy} - 2\Phi_x \Phi_y \Phi_{xy} + \Phi_y^2 \Phi_{xx})^{1/3}, \tag{23}$$

where κ is the Euclidean curvature of the level-sets of Φ, G is a Gaussian, and (23) is obtained from (22) via explicit computation of this curvature. The above equation means that each one of the level sets of Φ is evolving according to the affine heat flow developed in [33, 34] for planar shape smoothing, with the velocity "altered" by the function

$$\frac{1}{1 + \|\nabla(G * \Phi)\|}$$

as in [2] in order to reduce smoothing in the edges. This flow, and its Euclidean version (with κ instead of $\kappa^{1/3}$ in (22)), were tested in [1, 2, 35], and proved to give very satisfactory results. See the mentioned references for more details.

As we pointed out in the Introduction, the flows (7) and (22) can be combined to obtain a new flow which performs anisotropic diffusion (denoising) while simultaneously modifies the histogram. The flow is given by

$$\frac{\partial \Phi}{\partial t} = \frac{\alpha \kappa^{1/3} \|\nabla \Phi\|}{1 + \|\nabla (G * \Phi)\|} + (N^2 - H[\Phi(x, y, t)]) - \mathscr{A}[(v, w): \Phi(v, w, t) \geqslant \Phi(x, y, t)], \tag{24}$$

where $\alpha \in \mathbf{R}^+$ is a parameter which controls the trade-off between smoothing and histogram modification.

Other smoothing operators can be used as well. For instance, in [30] (see also [19] for theoretical results), the authors proposed to minimize the total variation of the image, given by

$$\int \|\nabla \Phi(X)\| \, dX.$$

It is easy to show that the Euler-Lagrange of this functional is given by the curvature κ of the level-sets, that is

$$\operatorname{div}\left(\frac{\nabla \Phi}{\|\nabla \Phi\|}\right) = \kappa,$$

which leads to the gradient descent flow

$$\Phi_t = \kappa.$$

Using this smoothing operator, together with the histogram modification part, gives very similar results as those obtained with the affine based flow. If this smoothing operator is combined with the histogram flow, the total flow

$$\frac{\partial \Phi}{\partial t} = \alpha \kappa + (N^2 - H[\Phi(x, y, t)]) - \mathscr{A}[(v, w): \Phi(v, w, t) \geqslant \Phi(x, y, t)] \tag{25}$$

will therefore be such that it reduces

$$\alpha \int \|\nabla \Phi(X)\| \, dX + \mathscr{U}, \tag{26}$$

where $\mathscr{U}$ is given by (20), obtaining a complete variational formulation[1] of the combined histogram-equalization/smoothing approach. This is precisely the formulation we analyze below.

[1] The affine flow has a variational interpretation as well, but much more complicated.

3.1. *Existence of the Flow*

We present now a theoretical result related to the simultaneous smoothing and contrast modification flow (25).

Before proceeding with the existence proof of the variational problem (26), let's recall the following standard notation:

1. $\mathscr{C}([0, T], \mathscr{H}) := \{\Phi: [0, T] \to \mathscr{H}$ continuous$\}$, where $T > 0$ and $\mathscr{H}$ is a Banach space (and in particular for a Hilbert space).

2. $L^p([0, T], \mathscr{H}) := \{\Phi: [0, T] \to \mathscr{H}$ such that $\int_0^T \|\Phi(t)\|^p < \infty\}$, with $1 \leqslant p < \infty$.

3. $L^\infty([0, T], \mathscr{H}) := \{\Phi: [0, T] \to \mathscr{H}$ such that $\operatorname{ess\,sup}_{t \in [0, T]} \|\Phi(t)\| < \infty\}$.

4. $\Phi \in L^p_{loc}([0, \infty), \mathscr{H})$ means that $\Phi \in L^p([0, T], \mathscr{H})$ for all $T > 0$.

5. $W^{1,2}([0, T], \mathscr{H}) := \{\Phi: [0, T] \to \mathscr{H}$ such that $\Phi, \Phi_t \in L^2([0, T], \mathscr{H})\}$.

In order to simplify notations, later we will assume $\Omega = (0, 1)^2$ and $\mathscr{H} = L^2(\Omega)$.

We proceed now to prove existence of the solution to the Euler–Lagrange equation corresponding to the variational problem (26), given by ($\alpha = 1$)

$$\Phi_t = \operatorname{div}\left(\frac{\nabla \Phi}{\|\nabla \Phi\|}\right) + \int_{[0, 1]^2} \operatorname{sign}^-(\Phi(t, Z) - \Phi(t, X))\, dZ - \Phi(t, X), \qquad (27)$$

together with the initial and boundary conditions

$$\Phi(0, X) = \Phi_0(X), \quad X \in [0, 1]^2, \qquad \frac{\partial \Phi}{\partial \vec{n}}(t, X) = 0, \quad t > 0, \ X \in \partial[0, 1]^2,$$

where $\vec{n}$ stands for the normal direction. We shall use results from the theory on non-linear semigroups on Hilbert space [4]. Before proceeding, we need a number of additional definitions. A function $\Phi \in L^1(\Omega)$ whose derivatives in the sense of distributions are measures with finite total variation in Ω, is called a function of bounded variation. The class of such functions will be denoted by $BV(\Omega)$. Thus, $\Phi \in BV(\Omega)$ if there are Radon measures $\mu_1, ..., \mu_n$ defined in $\Omega \subset \mathbf{R}^n$ such that its total mass $|D\mu_i|(\Omega)$ is finite and

$$\int_\Omega \Phi(X)\, D_i \phi(X)\, dX = -\int_\Omega \phi(X)\, d\mu_i(X)$$

for all $\phi \in \mathscr{C}_0^\infty(\Omega)$. The gradient of Φ will therefore be a vector valued measure with finite total variation

$$\|\nabla \Phi\| = \sup \left\{ \int_\Omega \Phi \operatorname{div} v \, dX : v = (v_1, ..., v_n) \in \mathscr{C}_0^\infty(\Omega, \mathbf{R}^n), |v(X)| \leqslant 1, X \in \Omega \right\}.$$

The space $\mathrm{BV}(\Omega)$ will have the norm

$$\|\Phi\|_{\mathrm{BV}} = \|\Phi\|_1 + \|\nabla \Phi\|.$$

The space $\mathrm{BV}(\Omega)$ is continuously embedded in $\mathrm{L}^p(\Omega)$ for all $p \leqslant n/(n-1)$. The inmersion is compact if $p < n/(n-1)$ ([37], Theorem 2.5.1). If Φ_i is a sequence of functions in $\mathrm{BV}(\Omega)$ converging to the function Φ in $\mathrm{L}^1(\Omega)$, then $\|\nabla \Phi\| \leqslant \lim_i \inf \|\nabla \Phi_i\|$ ([37], Theorem 5.2.1). Moreover, given a function $\Phi \in \mathrm{BV}(\Omega)$, there exists a sequence of functions $\Phi \in \mathrm{BV}(\Omega)$ such that $\Phi_i \to \Phi$ in $\mathrm{L}^1(\Omega)$ and such that $\|\nabla \Phi\| = \lim_i \|\nabla \Phi_i\|$ ([37], Theorem 5.2.3).

Let $\mathscr{H}$ be a Hilbert space and let $\phi: \mathscr{H} \to (-\infty, +\infty]$ be convex and proper. Given $X \in \mathscr{H}$, the subdifferential of ϕ at X, $\partial \phi(X)$, is given by

$$\partial \phi(X) = \{ Y \in \mathscr{H} : \forall \xi \in \mathscr{H}, \ \phi(\xi) - \phi(X) \geqslant \langle Y, \xi - X \rangle \}.$$

We write $\operatorname{dom}(\phi) := \{X \in \mathscr{H} : \phi(X) < +\infty\}$, $\operatorname{dom}(\partial \phi) := \{X \in \mathscr{H} : \partial \phi(X) \neq \varnothing\}$. From now on we shall write, as we mentioned before, $\Omega = (0, 1)^2$ and $\mathscr{H} = \mathrm{L}^2(\Omega)$. We also define the functionals $\phi, \psi: \mathscr{H} \to (-\infty, +\infty]$ by

$$\phi(\Phi) := \begin{cases} \|\nabla \Phi\| + \frac{1}{2} \int_\Omega (\Phi(X) - \frac{1}{2})^2 \, dX & \Phi \in \mathrm{BV}(\Omega) \\ +\infty & \text{otherwise,} \end{cases}$$

$$\psi(\Phi) := \tfrac{1}{4} \int_\Omega \int_\Omega |\Phi(Z) - \Phi(X)| \, dX \, dZ.$$

Note that both functionals are convex, lower semicontinuous, and proper on $\mathscr{H}$. We introduced both functionals since formally (27) is associated with the following abstract problem:

$$\Phi_t + \partial \phi(\Phi) \ni \partial \psi(\Phi). \tag{28}$$

To make such formulation precise, let us recall the following ([4], Definition 3.1): Let $T > 0$, $f \in \mathrm{L}^1([0, T], \mathscr{H})$. We call $\Phi \in \mathscr{C}([0, T], \mathscr{H})$ a strong solution of

$$\Phi_t + \partial \phi(\Phi) \ni f \tag{29}$$

is Φ is differentiable almost everywhere on $(0, T)$, $\Phi \in \mathrm{dom}(\partial\phi)$ a.e. in t and

$$-\Phi_t(t) + f(t) \in \partial\phi(\Phi(t)) \tag{30}$$

almost everywhere (a.e.) on $(0, T)$. In particular, if $\Phi \in W^{1,2}([0, T], \mathscr{H})$, $\Phi(t) \in \mathrm{dom}(\partial\phi)$ a.e. and (30) holds a.e. on $(0, T)$, then Φ is a strong solution of (29). We say that $\Phi \in \mathscr{C}([0, T], \mathscr{H})$ is a strong solution of (28) if there exists $\omega \in \mathrm{L}^1([0, T], \mathscr{H})$, $\omega(t) \in \partial\psi(\Phi(t))$ a.e. in $(0, T)$, such that Φ is a strong solution of

$$\Phi_t + \partial\phi(\Phi) \ni \omega. \tag{31}$$

With these preliminaries, we reformulate (27) as an abstract evolution problem of the form (28) and use the machinery of non-linear semigroups on Hilbert spaces to prove existence of solutions of (28).

THEOREM 2. *For any $\Phi_0 \in BV(\Omega)$, $0 \leqslant \Phi_0 \leqslant 1$, there exists a strong solution $\Phi \in W^{1,2}([0, T], \mathscr{H})$, $\forall T > 0$, of (28) with initial condition $\Phi(0) = \Phi_0$, and such that $0 \leqslant \Phi \leqslant 1$, $\forall t > 0$. Moreover, the functional $\mathscr{V}(\Phi) = \phi(\Phi) - \psi(\Phi)$ is a Lyapounov functional for (28).*

Proof. The proof is divided in a number of steps.

(1) *Regularization.* Define for each $\varepsilon > 0$, the following functionals

$$\phi_\varepsilon(\Phi) := \begin{cases} \dfrac{\varepsilon}{2}\int_\Omega \|\nabla\Phi\|^2\,dX + \dfrac{\varepsilon}{2}\int_\Omega \sqrt{\varepsilon^2 + \|\nabla\Phi\|^2}\,dX \\ \qquad + \dfrac{1}{2}\int_\Omega \left(\Phi(X) - \dfrac{1}{2}\right)^2 dX & \Phi \in \mathrm{BV}(\Omega) \\ +\infty & \text{otherwise,} \end{cases}$$

$$\psi_\varepsilon(\Phi) := \frac{1}{4}\int_\Omega\int_\Omega \beta_\varepsilon(\Phi(Z) - \Phi(X))\,dX\,dZ,$$

where $\beta_\varepsilon(r) := \sqrt{\varepsilon^2 + r^2}$, $r \in \mathbf{R}$. Observe that β_ε is smooth, β'_ε is an odd function, and $|\beta'_\varepsilon| \leqslant 1$. Both ϕ_ε and ψ_ε are convex, lower semicontinuous, and proper on $\mathscr{H}$. Let $\Phi_{\varepsilon 0} \in W^{1,2}(\Omega)$ be such that $0 \leqslant \Phi_{\varepsilon 0} \leqslant 1$, $\Phi_{\varepsilon 0} \to \Phi_0$ in $\mathscr{H}$, $\int_\Omega \|\nabla\Phi_{\varepsilon 0}\| \to \|\nabla\Phi_0\|$, and $\varepsilon\int_\Omega \|\nabla\Phi_{\varepsilon 0}\|^2 \to 0$ as $\varepsilon \to 0$. Hence $\phi_\varepsilon(\Phi_{\varepsilon 0}) \to \phi(\Phi_0)$ as $\varepsilon \to 0$ (such sequence exists from Lemma 3.1 in [11]). Since ϕ_ε is convex, lower semicontinuous, and proper, $\partial\phi_\varepsilon$ is a maximal monotone operator on $\mathscr{H}$ ([4], 2.3.4). On the other hand, letting

$$B_\varepsilon := \psi'_\varepsilon(\Phi) = -\tfrac{1}{2}\int_\Omega \beta'_\varepsilon(\Phi(Z) - \Phi(X))\,dZ, \qquad \Phi \in \mathscr{H}$$

$B_\varepsilon: \mathscr{H} \to \mathscr{H}$ satisfies

$$\|B_\varepsilon(\Phi) - B_\varepsilon(\hat{\Phi})\|_2 \leqslant \|\beta_\varepsilon''\|_\infty \|\Phi - \hat{\Phi}\|_2, \qquad \Phi, \hat{\Phi} \in \mathscr{H}.$$

That is B_ε is a Lipschitz operator on $\mathscr{H}$. Hence, $\partial\psi_\varepsilon + B_\varepsilon$ generates a strongly continuous semigroup on $\mathscr{H}$ ([4], Proposition 3.12). Therefore, there is a strong solution $\Phi_\varepsilon \in \mathscr{C}([0, T], \mathscr{H})$ of

$$\Phi_t + \partial\phi_\varepsilon(\Phi) + B_\varepsilon(\Phi) = 0$$

such that $\Phi_\varepsilon(0) = \Phi_{\varepsilon 0}$. Writing $f_\varepsilon(t) = -B_\varepsilon(\Phi_\varepsilon(t)) = \psi_\varepsilon'(\Phi_\varepsilon(t))$, $|f_\varepsilon| \leqslant \frac{1}{2}$. Therefore $f_\varepsilon \in \mathrm{L}^1([0, T], \mathscr{H})$ and we see that Φ_ε is a strong solution of

$$\Phi_t + \partial\phi_\varepsilon(\Phi) = f_\varepsilon \tag{32}$$

with $\Phi_\varepsilon(0) = \Psi_{\varepsilon 0}$. Since $\Phi_{\varepsilon 0} \in \mathrm{dom}(\phi_\varepsilon)$, using the regularization properties of semigroups generated by subdifferentials ([4], Theorem 3.6), we have the following estimates: $\Phi_\varepsilon \in W^{1,2}([0, T], \mathscr{H})$, $t \to \phi_\varepsilon(\Phi_\varepsilon(t))$ is absolutely continuous on $[0, T]$ and

$$\int_\Omega |\Phi_{\varepsilon t}|^2 + \frac{d}{dt}\phi_\varepsilon(\Phi_\varepsilon) = \langle f_\varepsilon, \Phi_{\varepsilon t}\rangle = \frac{d}{dt}\psi_\varepsilon(\Phi_\varepsilon). \tag{33}$$

In particular, from (33)

$$\int_\Omega |\Phi_{\varepsilon t}|^2 + \frac{d}{dt}\phi_\varepsilon(\Phi_\varepsilon) \leqslant \|f_\varepsilon\|_2 \|\Phi_{\varepsilon t}\|_2 \leqslant \frac{(\|f_\varepsilon\|_2)^2 + (\|\Phi_{\varepsilon t}\|_2)^2}{2}. \tag{34}$$

Integrating the equation above from 0 to T we obtain

$$\frac{1}{2}\int_0^T \int_\Omega |\Phi_{\varepsilon t}|^2 \, dX \, dt + \phi_\varepsilon(\Phi_\varepsilon) \leqslant \phi_\varepsilon(\Phi_{\varepsilon 0}) + \frac{T}{8}. \tag{35}$$

We have the following bounds independent of ε:

$$\int_\Omega \|\nabla\Phi_\varepsilon\| \leqslant M, \qquad \int_\Omega \|\Phi_\varepsilon\|^2 \leqslant M, \qquad \int_\Omega \|\Phi_{\varepsilon t}\|^2 \leqslant M, \tag{36}$$

$\forall t > 0$, $\forall \varepsilon > 0$, and some $M > 0$. The bounds above mean that $\Phi_\varepsilon \in W^{1,2}([0, T], \mathscr{H}) \cap \mathrm{L}^\infty([0, T], \mathrm{BV}(\Omega))$ for any $T > 0$.

(2) *Uniform bounds on* Φ_ε. To get the bounds $0 \leqslant \Phi_\varepsilon \leqslant 1$, let us observe that since ϕ_ε is strictly convex and ψ_ε is smooth, Φ_ε is the classical solution of the corresponding PDE

$$\Phi_t = \operatorname{div}\left(\varepsilon \nabla\Phi + \frac{\nabla\Phi}{\sqrt{\varepsilon^2 + \|\nabla\Phi\|^2}}\right) - \left(\Phi - \frac{1}{2}\right) - \frac{1}{2}\int_\Omega \beta'_\varepsilon(\Phi(t, Z) - \Phi(t, X))\, dZ. \tag{37}$$

It will be important to re-write (37) as

$$\Phi_t = \operatorname{div}\left(\varepsilon \nabla\Phi + \frac{\nabla\Phi}{\sqrt{\varepsilon^2 + \|\nabla\Phi\|^2}}\right) - \frac{1}{2}\int_\Omega (1 - \beta'_\varepsilon(\Phi(t, Z) - \Phi(t, X))\, dZ - \Phi. \tag{38}$$

To prove that $\Phi_\varepsilon \geqslant 0$, let $j \in \mathscr{C}^\infty(\mathbf{R})$, $j \geqslant 0$, $j' \leqslant 0$, $j'' \geqslant 0$, $j(r) = 0$ $\forall r \geqslant 0$, and $0 < j(r) \leqslant |r|$, $\forall r < 0$. Then

$$\frac{d}{dt}\int_\Omega j(\Phi_\varepsilon) = \int_\Omega j'(\Phi_\varepsilon)\, \Phi_{\varepsilon t}. \tag{39}$$

Based on (38), and integrating by parts, we obtain that the expression above is equal to

$$\int_\Omega j''(\Phi_\varepsilon)\, \nabla\Phi_\varepsilon \left[\varepsilon \nabla\Phi_\varepsilon + \frac{\nabla\Phi_\varepsilon}{\sqrt{\varepsilon^2 + \|\nabla\Phi_\varepsilon\|^2}}\right] dX + \frac{1}{2}\int_\Omega j'(\Phi_\varepsilon(t, X)) \int_\Omega (1 - \beta'_\varepsilon(\Phi_\varepsilon(t, Z) - \Phi_\varepsilon(t, X))\, dZ\, dX - \int_\Omega j'(\Phi_\varepsilon)\, \Phi_\varepsilon\, dX.$$

The first term is negative by definition. Since $|\beta'_\varepsilon| \leqslant 1$, and $j' \leqslant 0$, so is the second term. Since $j' \leqslant 0$ and $j(r) = 0$ for $r \geqslant 0$, the third term is negative as well. Hence, integrating (39) from 0 to T

$$\int_\Omega j(\Phi_\varepsilon(T, X))\, dX \leqslant \int_\Omega j(\Phi_\varepsilon(0, X))\, dX.$$

In particular, if $\Phi_\varepsilon(0) \geqslant 0$, $j(\Phi_\varepsilon) = 0$. Hence $\Phi_\varepsilon \geqslant 0$.

To prove that $\Phi_\varepsilon \leqslant 1$, let us compute for $p > 2$

$$\frac{d}{dt}\int_\Omega \Phi_\varepsilon(t, X)^p \, dX = p\int_\Omega \Phi_\varepsilon^{p-1}\Phi_{\varepsilon t}\, dX.$$

Using (38) and integrating by parts, this expression is equal to

$$-p(p-1)\int_\Omega \Phi_\varepsilon(t, X)^{p-2}\,\nabla\Phi_\varepsilon\left[\varepsilon\,\nabla\Phi_\varepsilon + \frac{\nabla\Phi_\varepsilon}{\sqrt{\varepsilon^2 + \|\nabla\Phi_\varepsilon\|^2}}\right] dX$$

$$+\frac{1}{2}p\int_\Omega \Phi_\varepsilon(t, X)^{p-1}\int_\Omega (1-\beta'_\varepsilon(\Phi_\varepsilon(t, Z)-\Phi_\varepsilon(t, X)))\, dZ\, dX$$

$$-p\int_\Omega \Phi_\varepsilon(t, X)^p\, dX.$$

It is clear that the first term is negative and the second term can be majorized using $(1-\beta'_\varepsilon) \leqslant 2$. Hence

$$\frac{d}{dt}\int_\Omega \Phi_\varepsilon(t, X)^p\, dX \leqslant p\int_\Omega \Phi_\varepsilon(t, X)^{p-1}\, dX - p\int_\Omega \Phi_\varepsilon(t, X)^p\, dX$$

$$\leqslant p\left(\int_\Omega \Phi_\varepsilon(t, X)^p\, dX\right)^{\frac{p-1}{p}} - p\int_\Omega \Phi_\varepsilon(t, X)^p\, dX,$$

where Hölder inequality has been used. Defining $\mathscr{A}_{\varepsilon p}(t) := (\int_\Omega \Phi_\varepsilon(t, X)^p\, dX)^{1/p}$, we have

$$\frac{d}{dt}\mathscr{A}_{\varepsilon p}(t)^p \leqslant p\mathscr{A}_{\varepsilon p}(t)^{p-1} - p\mathscr{A}_{\varepsilon p}(t)^p.$$

It follows that, where $\mathscr{A}_{\varepsilon p}(t) > 0$,

$$\frac{d}{dt}\mathscr{A}_{\varepsilon p}(t) \leqslant 1 - \mathscr{A}_{\varepsilon p}(t).$$

Then

$$\mathscr{A}_{\varepsilon p}(t) \leqslant 1 + \exp\{-t\}(\mathscr{A}_{\varepsilon p}(0) - 1).$$

If $p \to \infty$, $\mathscr{A}_{\varepsilon p}(t) \to \|\Phi_\varepsilon(t)\|_\infty$, $\mathscr{A}_{\varepsilon p}(0) \to \|\Phi_\varepsilon(0)\|_\infty$, and we have

$$\|\Phi_\varepsilon(t)\|_\infty \leqslant 1 + \exp\{-t\}(\|\Phi_\varepsilon(0)\|_\infty - 1) \leqslant 1.$$

Hence

$$0 \leqslant \Phi_\varepsilon \leqslant 1, \qquad \text{a.e.} \quad \forall \varepsilon > 0. \tag{40}$$

(3) *Letting* $\varepsilon \to 0$. From (36), we know that there exists a sequence Φ_ε such that $\Phi_\varepsilon \to \Phi$ in $L^1_{loc}([0, \infty) \times \bar{\Omega})$. From (40) we also have that $\Phi_\varepsilon \to \Phi$ in $L^p_{loc}([0, \infty) \times \bar{\Omega})$, $\forall p < \infty$, and $\Phi_\varepsilon \to \Phi$ weak-* in $L^\infty_{loc}([0, \infty) \times \bar{\Omega})$. Therefore,

$$\Phi \in W^{1,2}_{loc}([0, \infty), \mathscr{H}) \cap L^\infty_{loc}([0, \infty), \mathrm{BV}(\Omega)).$$

(The subindex "loc" could be omitted as we will see below). We also have $0 \leqslant \Phi \leqslant 1$ almost everywhere. Now, since Φ_ε is a strong solution of (32)

$$\phi_\varepsilon(\hat{\Phi}) - \phi_\varepsilon(\Phi_\varepsilon(t)) \geqslant \langle \Phi_{\varepsilon t}(t) - \psi'_\varepsilon(\Phi_\varepsilon(t)), \Phi_\varepsilon(t) - \hat{\Phi} \rangle, \qquad \forall \hat{\Phi} \in \mathscr{H}, \tag{41}$$

a.e. in t. Let $\mu_\varepsilon(t, Z, X) := \Phi_\varepsilon(t, Z) - \Phi_\varepsilon(t, X)$. Since $\mu_\varepsilon(t, Z, X) \to \Phi(t, Z) - \Phi(t, X)$ in $L^1_{loc}([0, \infty) \times \bar{\Omega})$, there exists a subsequence (call it again $\mu_\varepsilon(t, Z, X)$) such that $\beta'_\varepsilon(\mu_\varepsilon)$ converges to $s(t, X, Z) \in \mathrm{sign}(\Phi(t, Z) - \Phi(t, X))$ weakly-* in $L^\infty([0, T] \times \bar{\Omega})$ for all $T > 0$. Let $\omega := \int_\Omega s(t, Z, X)\, dZ$. We have

$$\langle \psi'_\varepsilon(\Phi_\varepsilon), \Phi_\varepsilon \rangle \to \langle \omega, \Phi \rangle, \qquad \langle \psi'_\varepsilon(\Phi_\varepsilon), \hat{\Phi} \rangle \to \langle \omega, \hat{\Phi} \rangle$$

weakly-* in $L^\infty([0, T])$ for all $T > 0$. Therefore, it also converges weakly in $L^1([0, T])$ for all $T > 0$. On the other hand, since $\Phi_\varepsilon \to \Phi$ in $L^2([0, T], \mathscr{H})$,

$$\langle \Phi_{\varepsilon t}, \Phi_\varepsilon \rangle = -\frac{1}{2} \frac{d}{dt} \langle \Phi_\varepsilon, \Phi_\varepsilon \rangle \to \frac{1}{2} \frac{d}{dt} \langle \Phi, \Phi \rangle$$

weakly in $L^1([0, T])$ for all $T > 0$. Similarly, $\langle \Phi_{\varepsilon t}, \hat{\Phi} \rangle \to \langle \Phi_t, \hat{\Phi} \rangle$ weakly in $L^1([0, T])$ for all $T > 0$. Finally, since $\phi(\Phi(t)) \leqslant \liminf_\varepsilon \phi_\varepsilon(\Phi_\varepsilon(t))$, $\phi(\hat{\Phi}) = \lim_\varepsilon \phi_\varepsilon(\hat{\Phi})$ for all $\hat{\Phi} \in W^{1,2}(\Omega)$, letting $\varepsilon \to 0$ in (41) we obtain

$$\phi(\hat{\Phi}) - \phi(\Phi(t)) \geqslant \langle \Phi_t(t) - \omega(t), \Phi(t) - \hat{\Phi} \rangle, \qquad \forall \hat{\Phi} \in W^{1,2}(\Omega),$$

a.e. in t. It follows that

$$\phi(\hat{\Phi}) - \phi(\Phi(t)) \geqslant \langle \Phi_t(t) - \omega(t), \Phi(t) - \hat{\Phi} \rangle, \qquad \forall \hat{\Phi} \in \mathscr{H},$$

a.e. in t. That is $\Phi(t) \in \mathrm{dom}(\partial\phi)$ and

$$-\Phi_t(t) + \omega(t) \in \partial\phi(\Phi(t)) \text{ a.e.}$$

To justify the last assertion of Theorem 1, let us observe that, from (32),

$$\frac{d}{dt}\left(\phi_\varepsilon(\Phi_\varepsilon(t)) - \psi_\varepsilon(\Phi_\varepsilon(t))\right) \leqslant 0.$$

Hence

$$\phi_\varepsilon(\Phi_\varepsilon(t)) - \psi_\varepsilon(\Phi_\varepsilon(t)) \leqslant \phi_\varepsilon(\Phi_\varepsilon(0)) - \psi_\varepsilon(\Phi_\varepsilon(0)) \text{ a.e.} \tag{42}$$

Since $\psi_\varepsilon(\Phi_\varepsilon(t)) \to \psi(\Phi(t))$, $\psi_\varepsilon(\Phi_\varepsilon(0)) \to \psi(\Phi(0))$, $\phi_\varepsilon(\Phi_\varepsilon(0)) \to \phi(\Phi(0))$, and ϕ is lower semicontinuous, we get $(\varepsilon \to 0)$

$$\phi(\Phi(t)) - \psi(\Phi(t)) \leqslant \phi(\Phi(0)) - \psi(\Phi(0)) \text{ a.e.} \tag{43}$$

Since Φ is a continuous function of t, we may assume that (43) holds for all t. Hence, $\phi - \psi$ is a Lyapounov functional for the problem (28). ∎

Note that the theorem above proves existence of a solution. There is no result so far related to uniqueness.

Before concluding this section, let us make some remarks on the asymptotic behavior of Φ as $t \to \infty$. Integrating (15) we have

$$\int_0^T \int_\Omega |\Phi_{\varepsilon t}|^2 \, dX \, dt = \phi_\varepsilon(\Phi_\varepsilon(t)) - \phi_\varepsilon(\Phi_\varepsilon(0)) + \psi_\varepsilon(\Phi_\varepsilon(t)) - \psi_\varepsilon(\Phi_\varepsilon(0))$$

$$\leqslant \phi_\varepsilon(\Phi_\varepsilon(0) + \tfrac{1}{4}.$$

Letting $\varepsilon \to 0$, we get

$$\int_0^T \int_\Omega |\Phi_t|^2 \, dX \, dt + \phi(\Phi(t)) \leqslant \psi(\Phi(0) + \tfrac{1}{4}.$$

Now, letting $T \to \infty$

$$\int_0^\infty \int_\Omega |\Phi_t|^2 \, dX \, dt \leqslant \psi(\Phi(0) + \tfrac{1}{4}.$$

Therefore, for a subsequence $t = t_n$ we have $\Phi_t(t_n) \to 0$ in $\mathscr{H}$ as $n \to \infty$. Since, on the other hand, $\phi(\Phi)$ is bounded, we may assume that $\Phi(t_n) \to \bar{\Phi}$ in L^1. Since $0 \leqslant \Phi \leqslant 1$, also $\Phi(t_n) \to \bar{\Phi}$ in L^2. Now, since $-\Phi_t + \omega \in \partial\phi(\Phi)$ a.e., we may assume that $-\Phi_t(t_n) + \omega(t_n) \in \partial\phi(\Phi(t_n))$ for all n. Hence

$$\phi(\hat{\Phi}) - \phi(\Phi(t_n)) \geqslant \langle -\Phi_t(t_n) + \omega(t_n), \Phi(t_n) - \hat{\Phi} \rangle, \qquad \forall \hat{\Phi} \in \mathscr{H}. \tag{44}$$

Moreover, we may assume that $\omega(t_n) \to \hat{\omega} \in \partial\psi(\hat{\Phi})$ weakly in $\mathscr{H}$. Letting $n \to \infty$ in the above expression, we get

$$\phi(\hat{\Phi}) - \phi(\bar{\Phi}) \geqslant \langle \bar{\omega}, \Phi - \hat{\Phi} \rangle \qquad \forall \hat{\Phi} \in \mathscr{H}.$$

In other words, $\hat{\omega} \in \partial\phi(\hat{\Phi})$ where $\hat{\omega} \in \partial\psi(\hat{\Phi})$. We may say that essentially all limit points of $\Phi(t)$ as $t \to \infty$ are critical points of $\phi(\Phi) - \psi(\Phi)$.

4. EXPERIMENTAL RESULTS

Before presenting experimental results, let us make some remarks on the complexity of the algorithm. Each iteration[2] of (7) (or (24)) requires $O(N^2)$ operations. In our examples we observed that no more than 5 iterations are usually required to converge. Therefore, the complexity of the proposed algorithm is $O(N^2)$, which is the minimal expected for any image processing procedure that operates on the whole image.

The first example is given in Fig. 4. The original image is presented on the top-left. On the right we present the image after histogram equalization performed using the popular software *xv*,[3] and on the bottom-left the one obtained from the steady state solution of (6). On the bottom-right we give an example of equation (7) for $h(\Phi)$ being a piece-wise linear function of the form $-\alpha(|\Phi - M/2| - M/2)$, where α is a normalization constant, Φ the image value, and M the maximal image value.

In Fig. 5 we show the progress of the histogram equalization flow. The original image is shown on the left, an intermediate step on the middle, and the steady state solution on the right.

An example of the simultaneous denoising and histogram equalization is given in Fig. 6 for a finger print image.[4]

Figure 7 presents an example of combining local and global histogram modification. The original image is given on the top left. The result of global histogram equalization on the top right, and the one for local contrast enhancement (16×16 neighborhood) on the bottom left. We see fronts appearing parallel to the edges. Finally, on the bottom right we show the combination of local and global contrast modification: we apply one (or several) global steps after k successive local steps. Note that the algorithm described in this paper is natural for this kind of combination, since all what is needed is the area $\mathscr{A}$ to be computed in a "time" dependent neighborhood.

[2] Note than in the case of just histogram modification, the explicit solution can be used in the implementation.

[3] Copyright 1993 by John Bradley.

[4] The image is from the database of the National Institute of Standards and Technology.

FIG. 4. Original image (top-left) and results of the histogram equalization process with the software package *xv* (top-right), the proposed image flow for histogram equalization (bottom-left), and the histogram modification flow for a piece-wise linear distribution (bottom-right).

FIG. 5. Progress of the histogram equalization flow. The original image is shown on the left, an intermediate step on the middle, and the steady state solution on the right.

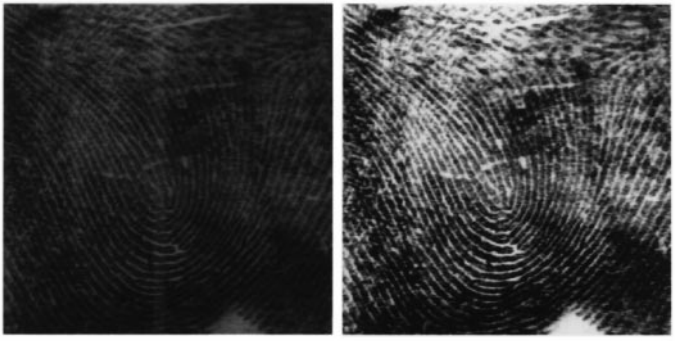

FIG. 6. Result (right) of simultaneous histogram equalization and anisotropic diffusion for a fingerprint image (left).

FIG. 7. Result of the combination of local and global contrast enhancement. The original image is given on the top left. The result of global histogram equalization on the top right, and the one for local contrast enhancement (16×16 neighborhood) on the bottom left. Finally, on the bottom right we show the combination of local and global contrast modification: The image on the left is further processed by the global histogram modification flow.

5. CONCLUDING REMARKS

In this paper, a novel framework for contrast enhancement via differential equations and variational formulations was presented. The modified image is obtained as the steady state solution of an image flow, which uses the original image as initial condition. The algorithm was tested on a number of images, and proved to converge very fast. Existence and uniqueness results, and a variational interpretation of the approach, were presented as well. The histogram modification flow can be combined with previously developed flows for anisotropic diffusion, in order to obtain a single PDE which simultaneously performs contrast normalization and denoising.

From the practical point of view, a number of issues have to be further investigated to improve the technique described in this paper. It is important to have a good understanding of the desired gray-value distributions for different applications. For example, the image in Fig. 3 looks very good for visual inspection, but it might be too saturated if the goal is to just make it "look nice." It is also necessary to define the structures that need to be preserved while improving the contrast. Another topic to be investigated is the use of metrics from the human visual system. Since these metrics include multi-scale, it is necessary to extend the variational formulation presented in this paper to multi-scale image representations. Finally, it would be interesting to extend the previous results to local contrast enhancement in the image space. These and other topics will be studied elsewhere.

In addition to the specific results described in this paper, we believe that the general framework here presented will help to answer very important open issues in image contrast enhancement.

ACKNOWLEDGMENTS

We thank Professor P. L. Lions from Paris IX-Dauphine and Professor P. Benilan from University of Besancon for stimulating discussions concerning this paper, Professor J. Blat from University of Illes Balears for his constant support, and the anonymous reviewer for suggestions that improved the presentation of the paper. VC acknowledges partial support by EC project MMIP-ERBCHRXCT930095 and DGICYT project PB94-1174.

REFERENCES

1. L. Alvarez, F. Guichard, P. L. Lions, and J. M. Morel, Axioms and fundamental equations of image processing, *Arch. Rational Mech.* **16** (1993), 200–257.
2. Lions L. Alvarez, P. L. Lions, and J. M. Morel, Image selective smoothing and edge detection by nonlinear diffusion, *SIAM J. Numer. Anal.* **29** (1992), 845–866.

3. L. Alvarez and L. Mazorra, Signal and image restoration by using shock filters and anisotropic diffusion, *SIAM J. Numer. Anal.* **31** (April 1994).
4. H. Brézis, "Operateurs maximaux monotones," Notes de Matematice, Vol. 50, North Holland Mathematical Studies, 1973.
5. V. Caselles, F. Catte, T. Coll, and F. Dibos, A geometric model for active contours, *Numerische Math.* **66** (1993), 1–31.
6. V. Caselles, R. Kimmel, and G. Sapiro, Geodesic active contours, *Int. J. Computer Vision*, to appear. (A short version appears in "Proc. Int. Conf. Comp. Vision '95," pp. 694–699, Cambridge, June 1995.)
7. A. Chambolle and P. L. Lions, Image recovery via total variation minimization and related problems, preprint, CEREMADE, University of Paris IX-Dauphine, 1995.
8. Y. G. Chen, Y. Giga, and S. Goto, Uniqueness and existence of viscosity solutions of generalized mean curvature flow equations, *J. Differential Geometry* **33** (1991), 749–786.
9. M. G. Crandall, H. Ishii, and P. L. Lions, User's guide to viscosity solutions of second order partial linear differential equations, *Bull. Amer. Math. Soc.* **27** (1992), 1–67.
10. L. C. Evans and J. Spruck, Motion of level sets by mean curvature, I, *J. Differential Geometry* **33** (1991), 635–681.
11. I. Ekeland and R. Teman, "Convex Analysis and Variational Problems," Studies in Mathematics and its Applications, North-Holland/Am. Elsevier, Amsterdam/New York, 1976.
12. M. Gage and R. S. Hamilton, The heat equation shrinking convex plane curves, *J. Differential Geometry* **23** (1986), 69–96.
13. D. Geman and G. Reynolds, Constrained restoration and the recovery of discontinuities, *IEEE Trans. PAMI* **14** (1992), 367–383.
14. G. Gerig, O. Kubler, R. Kikinis, and F. A. Jolesz, Nonlinear anisotropic filtering of MRI data, *IEEE Trans. Medical Imaging* **11** (1992), 221–232.
15. M. Grayson, The heat equation shrinks embedded plane curves to round points, *J. Differential Geometry* **26** (1987), 285–314.
16. S. Kichenassamy, A. Kumar, P. Olver, A. Tannenbaum, and A. Yezzi, Gradient flows and geometric active contour models, *in* "Proc. Int. Conf. Comp. Vision '95, Cambridge, June 1995," pp. 810–815.
17. B. B. Kimia, A. Tannenbaum, and S. W. Zucker, Shapes, shocks, and deformations, I, *Int. J. Computer Vision* **15** (1995), 189–224.
18. R. Kimmel and A. M. Bruckstein, Tracking level sets by level sets: A method for solving the shape from shading problem, *Computer Vision Image Understanding* **62**, No. 1 (1995), 47–58.
19. P. L. Lions, S. Osher, and L. Rudin, Denoising and debluring algorithms with constrained nonlinear PDEs, *SIAM J. Numer. Analysis*, in press.
20. R. Malladi and J. A. Sethian, Image processing: Flows under min/max curvature and mean curvature, *Graphical Models Image Process.* **58** (1996), 127–141.
21. R. Malladi, J. A. Sethian, and B. C. Vemuri, Shape modeling with front propagation: A level set approach, *IEEE Trans. PAMI* **17** (1995), 158–175.
22. S. J. Osher and J. A. Sethian, Fronts propagation with curvature dependent speed: Algorithms based on Hamilton-Jacobi formulations, *J. Comput. Phys.* **79** (1988), 12–49.
23. P. Olver, G. Sapiro, and A. Tannenbaum, "Affine Invariant Edge Maps and Active Contours," Geometry Center Technical Report 90, University of Minnesota, October 1995.
24. S. Osher and L. I. Rudin, Feature-oriented image enhancement using shock filters, *SIAM J. Numer. Anal.* **27** (1990), 919–940.
25. E. J. Pauwels, P. Fiddelaers, and L. J. Van Gool, Shape-extraction for curves using geometry-driven diffusion and functional optimization, *in* "Proc. Int. Conf. Comp. Vision '95, Cambridge, June 1995," pp. 396–401.

26. P. Perona and J. Malik, Scale-space and edge detection using anisotropic diffusion, *IEEE Trans. Pattern Anal. Machine Intell.* **12** (1990), 629–639.
27. P. Perona and M. Tartagni, Diffusion network for on-chip image contrast normalization, *in* "Proc. IEEE-International Conference on Image Proc. 1, Austin, Texas, November 1994," pp. 1–5.
28. W. K. Pratt, "Digital Image Processing," Wiley, New York, 1991.
29. E. Rouy and A. Tourin, A viscosity solutions approach to shape-from-shading, *SIAM J. Numer. Anal.* **29** (1992), 867–884.
30. L. I. Rudin, S. Osher, and E. Fatemi, Nonlinear total variation based noise removal algorithms, *Physica D* **60** (1992), 259–268.
31. G. Sapiro, Geometric partial differential equations in image processing: Past, present, and future, *in* "Proc. Second IEEE-International Conference on Image Processing 3, Washington DC, October 1995," pp. 1–4.
32. G. Sapiro, R. Kimmel, D. Shaked, B. B. Kimia, and A. M. Bruckstein, Implementing continuous-scale morphology via curve evolution, *Pattern Recog.* **26** (1993), 1363–1372.
33. G. Sapiro and A. Tannenbaum, On affine plane curve evolution, *J. Functional Anal.* **119** (1994), 79–120.
34. G. Sapiro and A. Tannenbaum, Affine invariant scale-space, *Int. J. Computer Vision* **11** (1993), 25–44.
35. G. Sapiro, A. Tannenbaum, Y. L. You, and M. Kaveh, Experiments on geometric image enhancement, *in* "Proc. First IEEE-International Conference on Image Processing 2, Austin-Texas, November 1994," pp. 472–476.
36. R. T. Whitaker and S. M. Pizer, A multi-scale approach to nonuniform diffusion, *CVGIP: Image Understand.* **51** (1993), 99–110.
37. W. P. Ziemer, "Weakly Differentiable Functions," Springer-Verlag, Berlin, 1989.